JOURNAL OF CATALYSIS 21, 282–293 (1971)

Oxidative Dehydrogenation of Butenes over Ferrite Catalysts

R. J. RENNARD AND W. L. KEHL

Gulf Research & Development Company, Pittsburgh, Pennsylvania 15230

Received July 17, 1970

Catalysts consisting of zinc-chromium ferrite and magnesium-chromium ferrite have been studied for the oxidative dehydrogenation of butene-2 to butadiene. These catalysts have a spinel structure with Cr^{+3} replacing Fe^{+3} in octahedral sites. The substitution of chromium for iron (in the spinel) greatly increases the efficiency of the catalyst for oxidative dehydrogenation and stabilizes the catalyst against bulk reduction in a hydrocarbon atmosphere. Data for both oxidative dehydrogenation and butene isomerization indicate that the reaction proceeds via an allylic intermediate. The dehydrogenation reaction involves two oxygen species, an adsorbed oxygen ion and an O^{-2} lattice oxygen. Mössbauer spectra and magnetic susceptibilities are discussed along with effects of varying the chromium concentration on the physical properties and catalytic activity of these spinels.

INTRODUCTION

The oxidative dehydrogenation of butene to butadiene has become an important commercial process, and superior catalysts consisting of zinc–chromium ferrites and magnesium–chromium ferrites have been developed for this process (*1*, *2*). Both catalysts exhibit a high activity and selectivity for this reaction. These catalysts have the $A^{+2}B_2^{+3}O_4$ spinel type structure. Within this structure three different forms are possible. These forms, which are shown in Table 1, are: (1) a normal spinel in which the divalent cations are in tetrahedral sites and the trivalent cations are in octahedral sites; (2) an inverse spinel in which the divalent cations are in octahedral sites, and the trivalent cations are distributed half in tetrahedral sites and half in octahedral sites; (3) a random spinel in which divalent and trivalent cations are distributed in both tetrahedral and octahedral sites. $MgCrFeO_4$ has the random structure except that Cr^{+3} always occupies octahedral sites. The addition of Cr^{+3} to form compounds of $ZnCr_xFe_{2-x}O_4$ results in the replacement of Fe^{+3} in octahedral sites with Cr^{+3}. On the other hand, the addition of Cr^{+3} to form compounds of the type $MgCr_xFe_{2-x}O_4$ results in the rearrangement of both Mg^{+2} and Fe^{+3} cation distributions since Cr^{+3} goes into octahedral sites occupied by both Mg^{+2} and Fe^{+3}. It is possible to vary the structure over the complete range from normal to random to inverse as x goes from 0 to 2 in $MgCr_xFe_{2-x}O_4$. This does not happen in the system $ZnCr_xFe_{2-x}O_4$ which has the normal spinel structure over the entire range of x from

TABLE 1
SPINEL CATALYSTS

Type	Structure	Examples
Normal	$(A^{+2})[B_2^{+3}]O_4$	$ZnFe_2O_4$ $ZnCrFeO_4$ $ZnCr_2O_4$ $MgCr_2O_4$
Inverse	$(B^{+3})[A^{+2}B^{+3}]O_4$	$MgFe_2O_4$
Random	$(A_x^{+2}B_y^{+3})[A^{+2}{}_{1-x}B^{+3}{}_{2-y}]O_4$	$MgCrFeO_4$

0 to 2. Therefore, differences in both the catalytic activity and physical properties would be expected as the chromium to iron ratio is varied in the $MgCr_xFe_{2-x}O_4$ systems. Variation of the chromium to iron ratio in the $ZnCr_xFe_{2-x}O_4$ system, on the other hand, would be expected to have a lesser effect on the catalytic behavior.

The following is a summary of some of the results obtained in a study of the catlytic properties of the zinc and magnesium–chromium ferrites for the oxidative dehydrogenation of butenes.

Experimental

Catalysts were prepared by coprecipitation from the nitrate salts with NH_4OH or NaOH. Detailed methods of preparation of the zinc and magnesium–chromium ferrites are given in the patent literature (*1*, *2*). The binary ferrites were precipitated at room temperature in either NH_4OH or NaOH. After filtering and washing, the catalysts were dried at 120°C for 16 hr, then calcined for 16 hr at the desired temperature (usually 650°C).

Catalyst evaluations were carried out in a stainless steel flow reactor, using pure oxygen as the oxidant and steam as the inert carrier gas. Blank runs at reaction temperatures showed no reaction in the absence of catalyst. Experiments performed in stainless steel, quartz-lined stainless steel, and quartz-tube reactors showed no measurable effect of reactor material on catalytic activity. All reactants were reagent grade and used without further purification.

After calcination, all catalysts were analyzed by X-ray diffraction using CuK_α radiation and a gas proportional counter with pulse amplitude discrimination to minimize background due to fluorescence. The stoichiometry of each preparation was verified by X-ray fluorescence analysis, and surface areas were determined by standard BET nitrogen adsorption.

Before catalytic activity measurements were made all catalysts were given a standard pretreatment consisting of a 30-min. oxidation in a flow of steam and oxygen at a 10 to 1 mole ratio and a GHSV of 6600 hr^{-1} at 500°C, followed by reduction in a flow of steam and butene in a 10 to 1 molar ratio at GHSV of 6600 hr^{-1} at 500°C.

Initial testing was carried out under essentially adiabatic conditions, and analyses were carried out by on-stream GLC after the reaction had reached a steady-state.

Results

Zinc Spinel Catalysts

Table 2 shows the composition and structural features of the different catalysts used in this study. All of the catalysts with the exception of the freshly calcined zinc–chromium ferrites were well crystallized, single-phase compounds. The oxidation state of the iron in the catalysts was determined to be Fe^{+3}, as will be shown later.

TABLE 2
Description of Catalysts

Catalyst	Composition	Surface area (m^2/g)
$ZnCrFeO_4$	Major spinel phase Minor $(FeCr)O_3$ and ZnO	11
$ZnCr_{.25}Fe_{1.75}O_4$	Major spinel phase Minor $(FeCr)O_3$	10
$ZnCr_{.1}Fe_{1.9}O_4$	Major spinel phase Minor $(FeCr)O_3$	10
$ZnFe_2O_4$	Single-phase spinel	10
α-$FeCrO_3$	Single-phase $(FeCr)O_3$	11
α-Fe_2O_3	Single-phase (α-Fe_2O_3)	10
$ZnCr_2O_4$	Single-phase spinel	26

Table 3 shows data obtained under adiabatic conditions for the oxidative dehydrogenation of butene-2 over the various catalysts listed in Table 2. All of these catalysts, with the exception of the zinc chromite, show selectivity for the formation of butadiene. However, the α-Fe_2O_3 shows selectivity only at lower temperatures. Attempts to increase the yield of butadiene by increasing temperature or oxygen pressure resulted in a drastic loss in selectivity. The same is true for α-$FeCrO_3$ but to a lesser degree. The $ZnFe_2O_4$ shows a high selectivity but a lower activity than any of the iron containing catalysts. The zinc–chromium ferrite catalysts all show both

TABLE 3

COMPARATIVE DATA FOR THE OXIDATIVE DEHYDROGENATION OF BUTENE-2 TO BUTADIENE, GHSV = 450 AND $\frac{\text{STEAM}}{C_4H_8} = 10$

Catalyst	T°C	O_2/C_4	Conversion (mole %)	Selectivity to C_4H_6 (mole %)	Yield C_4H_6 (mole %)
$ZnCrFeO_4$	325	.67	58	91	53
$ZnCr_{.25}Fe_{1.75}O_4$	325	.67	56	90	50
$ZnCr_{.1}Fe_{1.9}O_4$	325	.67	46	92	42
$ZnFe_2O_4$	325	.67	20	89	18
	375	.67	47	88	41
α-$FeCrO_3$	325	.67	50	84	43
	375	1	57	76	43
α-Fe_2O_3	325	.67	35	83	29
	375	1.00	23	43	11
$ZnCr_2O_4$	325	.67	15	16	2

a high activity and high selectivity to butadiene. The effect of varying the chromium concentration in $ZnCr_xFe_{2-x}O_4$ from $x = 1$ to $x = 0$ has very little effect on the selectivity to butadiene, but conversion decreases as the chromium content decreases.

Since the $FeCrO_3$ catalyst shows high activity, and all three of the fresh zinc–chromium ferrite catalysts contain minor amounts of a $Cr_xFe_{2-x}O_3$ phase, the possibility was raised that the higher activity of the chromium containing zinc ferrite is due not to incorporation of Cr^{+3} into the spinel lattice but to the presence of the $Cr_xFe_{2-x}O_3$ phase. However, X-ray diffraction analysis of the used zinc–chromium ferrites showed that this $Cr_xFe_{2-x}O_3$ phase had disappeared completely, and only a well-crystallized single-phase spinel was present. X-Ray analysis also showed that the amount of this $Cr_xFe_{2-x}O_3$ phase decreases as the temperature of calcination increases.

These results indicate that the diffusion of the Cr^{+3} and Fe^{+3} from the $Cr_xFe_{2-x}O_3$ phase into the spinel lattice occurs more readily in the presence of hydrocarbon than in air. Quite likely this occurs during the reduction step of the catalyst pretreatment. The effect of this reduction on the catalytic activity of these catalysts is shown in Table 4. Both of the zinc–chromium ferrite catalysts show an increase in activity after reduction, whereas this reduction has no effect on the activity of the $ZnFe_2O_4$ catalyst. Here again the freshly calcined zinc–chromium ferrites contain a minor $Cr_xFe_{2-x}O_3$ phase, which is not present in the used catalyst. It is quite certain then that the $Cr_xFe_{2-x}O_3$ phase in the fresh zinc–chromium ferrites is not responsible for their high activity,

TABLE 4

EFFECT OF PREREDUCTION ON ZINC CONTAINING FERRITES

Catalyst	Pretreatment	T°C	O_2/C_4	Conversion (mole %)	Yield C_4H_6 (mole %)
$ZnCrFeO_4$	Fresh calcined no reduction	400	(1)	60	46
$ZnCrFeO_4$	Fresh calcined reduced in butene 500°C	400	(1)	70	58
$ZnCr_{.25}Fe_{1.75}O_4$	Fresh calcined no reduction	400	(1)	61	46
$ZnCr_{.25}Fe_{1.75}O_4$	Fresh calcined reduced in butene 500°C	400	(1)	71	58
$ZnFe_2O_4$	Fresh calcined no reduction	400	(1)	62	48
$ZnFe_2O_4$	Fresh calcined reduced in butene 500°C	400	(1)	60	47

but this activity is due to the incorporation of Cr^{+3} into the spinel lattice. In order to gain more information into the nature of the disappearance of the $Cr_xFe_{2-x}O_3$ phase, magnetic susceptibility measurements were made on a $ZnCrFeO_4$ catalyst calcined at different temperatures along with a used $ZnCrFeO_4$ catalyst initially calcined at 500°C.

The results of these measurements are presented in Fig. 1 which shows the saturation moment as a function of applied magnetic field strength. It is obvious that the saturation moment, although quite small for all of the catalysts, increases with calcination temperature for the fresh catalysts, and the moment for the used catalyst is even higher than that for the catalyst calcined at 1000°C. The used catalyst was not exposed to a temperature over 500°C during use.

Indirect exchange mechanisms which produce spontaneous magnetization in spinels have been the subject of extensive studies, and the suggestion has been made

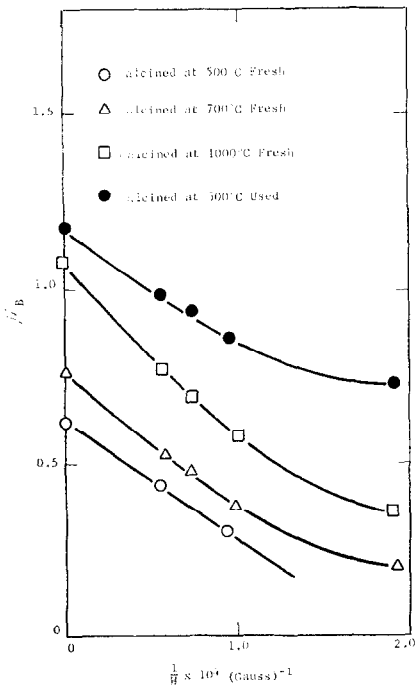

FIG. 1. A plot of saturation moment, in μ_B, vs the applied magnetic field strength showing the effect of calcination temperature and hydrocarbon atmosphere on the $ZnCrFeO_4$ catalyst.

by Wickham and Goodenough (*3*) that direct interactions between octahedral site cations are possible under certain conditions. These conditions are related to the extent to which the A-site and the B-site t_2^g and e_g orbitals of the involved cations are filled. In the case of Cr^{+3} and Fe^{+3}, the conditions are precisely those postulated for strong B–B interactions. These B–B interactions would tend to increase as the $Cr_xFe_{2-x}O_3$ phase disappears by diffusion into the spinel lattice, with a resultant increase in saturation moment. Thus, the magnetic susceptibility measurements support the earlier conclusion that the diffusion of the $Cr_xFe_{2-x}O_3$ phase into the spinel lattice is facilitated in a hydrocarbon atmosphere.

Magnesium Spinel Catalysts

Table 5 shows data obtained for the oxidative dehydrogenation of butene-2 to butadiene over a series of magnesium spinel catalysts along with data for α-$FeCrO_3$ and α-Fe_2O_3. These data were obtained under the same conditions as described for the zinc spinels. Again it can be seen that the magnesium chromite shows very little selectivity for butadiene. The increase in activity when half of the iron in $MgFe_2O_4$ is replaced with chromium is not as marked as for the similar substitution in zinc ferrite. However, $MgCrFeO_4$ is significantly more active than $MgFe_2O_4$ under the same conditions.

In the $MgCr_xFe_{2-x}O_4$ system varying x from 0 to 2 has a profound effect on the structure of the catalyst in that the chromium replaces both magnesium and iron in octahedral sites. It would be expected that varying the chromium to iron ratio would also have a significant effect on the catalytic properties of this system. A series of magnesium–chromium ferrites was prepared in which x was varied from 0 to 1.75. The distribution of Fe^{+3} and Mg^{+2} in tetrahedral sites of the spinel lattice (for each catalyst) was determined from analyses of the relative intensities of the lines in the X-ray diffraction powder patterns. In Fig. 2 the catalytic activity and the fraction γ of the Fe^{+3} occupying tetrahedral sites is plotted as a function of x in

TABLE 5
COMPARATIVE DATA FOR THE OXIDATIVE DEHYDROGENATION OF BUTENE-2 TO BUTADIENE

Catalyst	T°C	O_2/C_4	Conversion (mole %)	Selectivity C_4H_6 (mole %)	Yield C_4H_6 (mole %)
$MgCrFeO_4$	325	.67	64	90	58
$MgFe_2O_4$	325	.67	53	86	46
α-$FeCrO_3$	325	.67	50	84	43
α-Fe_2O_3	325	.67	35	83	29
$MgCr_2O_4$	325	1	28	32	9

$MgCr_xFe_{2-x}O_4$. Catalytic activity is expressed in terms of first-order rate constants, k, for the production of butadiene which have been normalized to a standard surface area. The drastic change in activity with x is quite evident. The reason for the maximum in activity at $x = \frac{1}{2}$ is not understood. Such a maximum does not occur in the zinc–chromium ferrite system. Although the magnesium–chromium ferrite and zinc–chromium ferrite systems differ in this respect, the catalytic properties of the compositions $ZnCrFeO_4$ and $MgCrFeO_4$ are surprisingly similar. They differ in relative activity but show the same selectivities, product distribution and the same temperature dependence.

Mössbauer Studies

Mössbauer spectra were obtained at room temperature for selected samples of these ferrite catalysts. The source was Co^{57} in chromium, and an NBS sample of sodium nitroprusside was used as a calibration standard.

A Mössbauer spectrum can provide information concerning (1) the valence state of the nuclide, in this case Fe; (2) the electric field gradient, if any, at the site of the nuclide; and (3) the strength of the magnetic field at the nucleus. The valence state is deduced from the magnitude of the isomer shift, S, and an electric field gradient at the site of the nuclide is manifested

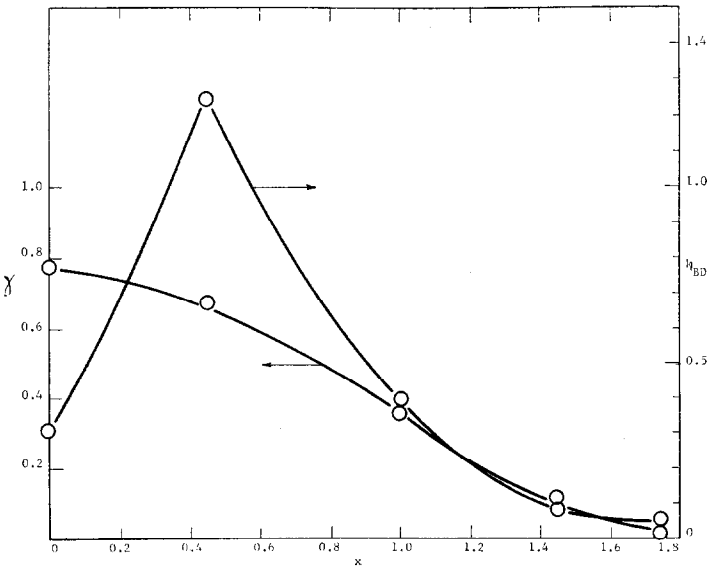

FIG. 2. Fraction Fe^{+3} in tetrahedral sites and rate constants for the formation of butadiene as a function of x in $MgCr_xFe_{2-x}O_4$.

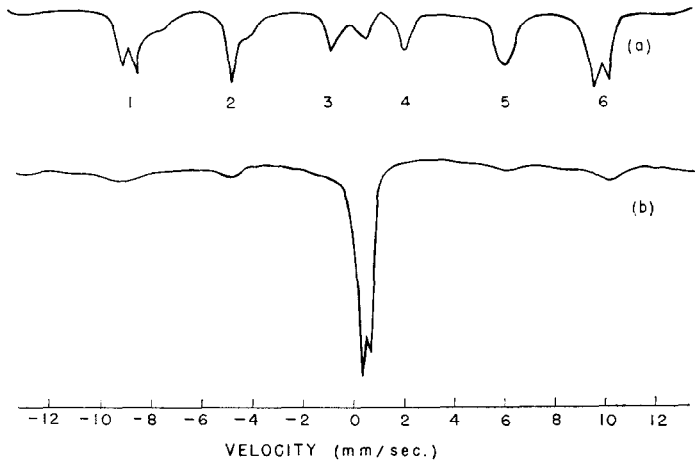

FIG. 3. Room temperature Mössbauer spectra of used samples of (a) $MgFe_2O_4$, and (b) $ZnFe_2O_4$.

by a quadrupole splitting, ΔE, of the resonance absorption line. The presence of a magnetic field at the nucleus produces a Zeeman splitting of the nuclear energy levels and this results in hyperfine structure in the Mössbauer spectrum. The positions of the hyperfine lines can be used to calculate the strength, H, of the magnetic field experienced by the nucleus.

The room temperature spectra of $MgFe_2O_4$ and $ZnFe_2O_4$ after use for the oxidative dehydrogenation of butenes are shown in Fig. 3, and the corresponding spectra for $FeCrO_3$, $MgCrFeO_4$ and $ZnCrFeO_4$ are shown in Fig. 4. The isomer shift, quadrupole splitting, and magnetic field at the nucleus were calculated for these five samples, and the results are summarized in Table 6. Data from the literature for bulk α-Fe_2O_3 also are included for comparison.

It has been shown (*4*) that for well-characterized ferric ions, the isomer shift is approximately 0.5 mm/sec, and on this basis it is clear from Table 6 that the iron is present as Fe^{+3} in all of these catalysts. The quadrupole splitting data shown in column 3 were calculated from the central

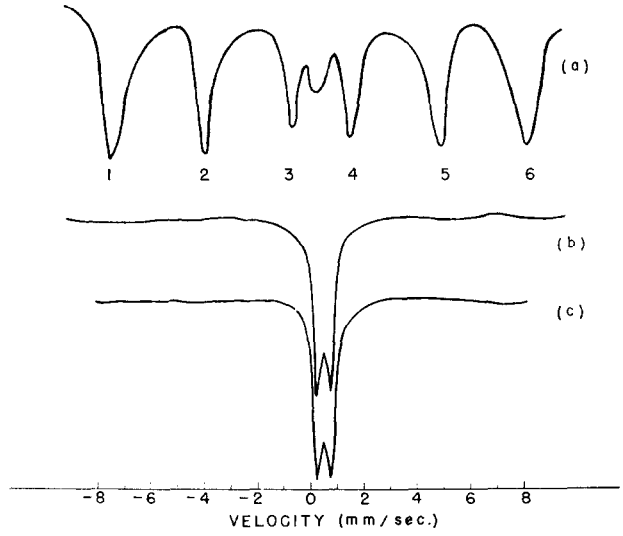

FIG. 4. Room temperature Mössbauer spectra of used catalysts (a) $(Fe,Cr)_2O_3$, (b) $ZnCrFeO_4$, and (c) $MgCrFeO_4$.

TABLE 6

ISOMER SHIFT, QUADRUPLE SPLITTING, AND MAGNETIC FIELD AT THE IRON NUCLEUS AS DETERMINED FROM THE MÖSSBAUER SPECTRA OF FERRITE CATALYSTS

Catalyst	Isomer shift (mm/sec)	Quadrupole splitting (mm/sec)	Magnetic field at nucleus, H (oersteds)
α-Fe_2O_3	0.5	—	5.17×10^5
α-$(Fe,Cr)_2O_3$	0.45	(a)	4.21×10^5
$ZnFe_2O_4$	0.5	0.3	5.7×10^5
$MgFe_2O_4$[a]	0.5	—	5.65×10^5
			5.36×10^5
			$\simeq 4.84 \times 10^5$
$ZnCrFeO_4$ (used)	0.48	0.36	Not observed
$MgCrFeO_4$ (used)	0.54	0.57	Not observed

[a] Quadrupole splitting for $MgFe_2O_4$ not measured (inadequate resolution).

line which corresponds to a phase in which the energy levels are not subject to Zeeman splitting. The results show that the electric field gradient at the iron atoms is the same in the two zinc-containing samples, and is smaller than in $MgCrFeO_4$. The central line of the spectra of the remaining two samples apparently was a doublet also, but the resolution was not adequate to permit a determination of the quadrupole splitting.

The magnetic field strength, H, at the iron nucleus was calculated from the separation of the two outermost lines of the hyperfine spectrum, and the calculation was based on the value 3.3×10^5 oersteds for metallic iron (*5*). The nature and intensity of the hyperfine spectrum varies widely among these samples, as illustrated in Figs. 3 and 4. In $ZnFe_2O_4$, the magnetic phase is only a minor component, while in $MgFe_2O_4$, it is the major component, and iron nuclei are located in at least three different types of site. It also is worth noting that in α-$FeCrO_3$, which has the same type of crystal structure as α-Fe_2O_3, the principal phase is magnetic, but the magnetic field H is much weaker than in α-Fe_2O_3. The hyperfine lines of this spectrum are asymmetric on the low velocity side, and this indicates that some of the iron nuclei are located in sites where the magnetic field is even weaker than that indicated in Table 6.

The room-temperature spectra of used $ZnCrFeO_4$ and $MgCrFeO_4$ catalysts are nearly identical. The substitution of Cr^{+3} for one-half of the Fe^{+3} in the $MgFe_2O_4$ structure has a very pronounced effect, but this effect is much less pronounced when a similar substitution is made in the $ZnFe_2O_4$ lattice. The similarity and nature of the room-temperature spectra for $ZnCrFeO_4$ and $MgCrFeO_4$ suggest that in both cases the introduction of Cr^{+3} into the structure reduces the magnetic domain size to the point where superparamagnetic behavior (*6*, *7*) is observed. If this is the case, then low temperature Mössbauer spectroscopy, at temperatures where the superparamagnetism disappears, should disclose the exact role of the Cr^{+3} in the two different catalysts. These experiments have not been completed.

Isomerization of Unreacted Butene-2

Early in the study of the oxidative dehydrogenation of butene-2 over the zinc and magnesium–chromium ferrites, it was noted that the unreacted butenes contained only small amounts of butene-1. In all cases the mole fraction of butene-1 was well below the calculated equilibrium values as illustrated in Table 7 which lists typical data showing the extent of isomerization vs conversion to butadiene for both zinc–chromium ferrite and magnesium–chromium ferrite. Under normal reaction conditions, the amounts of butene-1 were always substantially less than 50% of equilibrium. These results suggest that rapid isomerization is occurring, but the butene-1 formed is being preferentially converted to buta-

TABLE 7
ISOMERIZATION AND BUTADIENE YIELD FOR THE OXIDATIVE DEHYDROGENATION OF BUTENE-2 OVER $ZnCrFeO_4$ AND $MgCrFeO_4$

Catalyst	T°C	Yield C_4H_6 (mole %)	Butene-1 (mole %)	Equilibrium butene-1 (mole %)
$ZnCrFeO_4$	325	20.7	4.5	14.9
	350	45.4	6.8	16.0
	375	59.7	8.1	17.2
$MgCrFeO_4$	325	10.4	2.6	14.9
	350	30.6	6.2	16.0
	375	46.0	7.6	17.2

diene, so that the concentration of butene-1 would be expected to be less than equilibrium. If this were the case, the oxidative dehydrogenation of butene-1 to butadiene should occur at a faster rate than the conversion of butene-2. To test this, a series of experiments was carried out isothermally over $ZnCrFeO_4$ catalysts alternately using butene-1 and butene-2 as the reactant. Representative results of these experiments are listed in Table 8. At both high and low butene conversion, the yield of butadiene is the same regardless of whether butene-1 or butene-2 is used as reactant. Again regardless of whether butene-1 or butene-2 is used the amount of the double-bond isomer found in the unreacted butenes is far less than the calculated equilibrium values. This suggests that the oxidative dehydrogenation of both butene-1 and butene-2 over these catalysts proceeds via the same intermediate, and that under reaction conditions the rate of dehydrogenation is faster than the rate of isomerization.

TABLE 8
COMPARATIVE DATA FOR THE OXIDATIVE DEHYDROGENATION OF BUTENE-1 AND BUTENE-2 OVER $ZnCrFeO_4$

T°C	Feed	Yield C_4H_6 (mole %)	Isomer (mole %)	Equilibrium isomer (mole %)
325	Butene-1	14.6	16.1[a]	85.1
325	Butene-2	14.7	2.6[b]	14.9
350	Butene-1	49.5	24.6[a]	84.0
350	Butene-2	50.0	8.3[b]	16.0

[a] Butene-2 formed from butene-1.
[b] Butene-1 formed from butene-2.

Reactions in the Absence of Oxygen

It has been reported that butene may be dehydrogenated to butadiene over some oxide catalysts in the absence of oxygen by reaction with lattice oxygen and subsequent bulk reduction of the catalyst (*8*, *9*). A series of experiments was conducted in the absence of oxygen over both the zinc and magnesium–chromium ferrite catalysts. These experiments were carried out at 360 and 460°C in a 10 to 1 steam to butene atmosphere with a butene GHSV of 600 hr^{-1}. Before each experiment, the catalyst was treated with a 10 to 1 steam to oxygen stream at 500°C for 30 min. At 360°C for both butene-1 and butene-2, butadiene and CO_2 were formed in small amounts for the first few minutes of reaction. After a few minutes, the CO_2 disappeared. The initial product contained 2 mole % butadiene and fell to zero within a maximum of 40 min. Isomerization of the butenes occurred over the entire period and approached steady-state after 40 min. The steady-state yields of CO_2, butadiene and double-bond isomerization at 360°C are shown in Table 9.

TABLE 9
REACTION IN THE ABSENCE OF OXYGEN OVER $ZnCrFeO_4$

T°C	Feed	C_4H_6 (mole %)	CO_2 (mole %)	Isomer (mole %)
360	Butene-2	0	0	12.1
360	Butene-1	.5	0	33.3
460	Butene-2	3.3	.2	27.8
460	Butene-1	3.9	.3	72.1
460[a]	Butene-2	2.8	.1	21.8

[a] $MgCrFeO_4$.

Figure 5 is a plot of butadiene and butene-1 formed in the reaction of butene-2 over $ZnCrFeO_4$ in the absence of oxygen at 360°C vs time. The yield of CO_2 is too low to appear in this plot. Since, due to the sampling technique, the points at 2 min

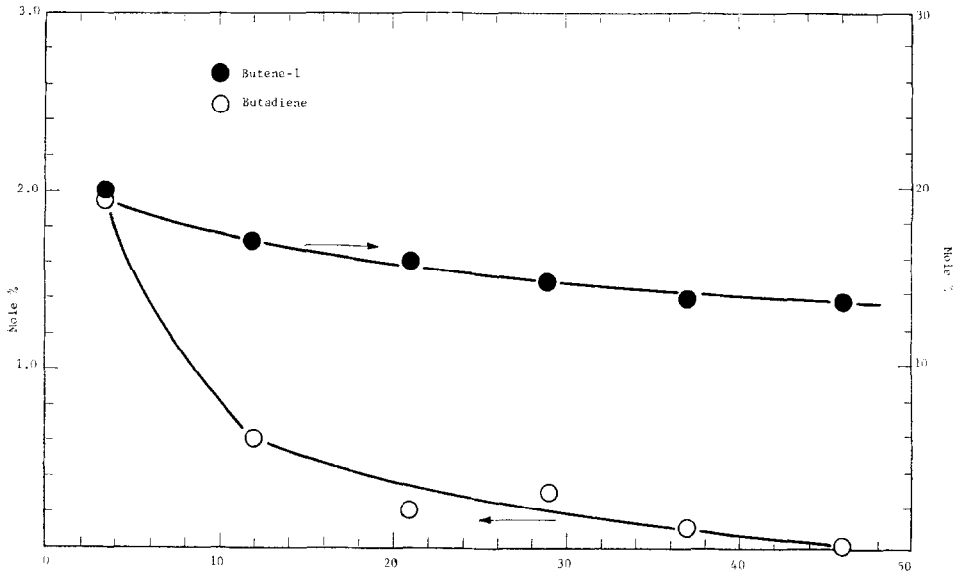

FIG. 5. Reaction of butene-2 over $ZnCrFeO_4$ in the absence of oxygen at 360°C.

represent the initial reaction products formed, it is possible from these data to estimate the total amount of oxygen consumed in the formation of these products. For both butene-1 and butene-2, the total oxygen consumed is equivalent to 1 to 2 monolayers based on the surface area of the catalyst. It thus appears that when the loosely bound surface oxygen is removed the oxidative reaction ceases, and there is no *bulk* reduction of the catalyst.

These experiments were repeated at 460°C. At this temperature any bulk reduction should be rapid and quantitatively measureable.

As shown in Table 9 small but significant amounts of both CO_2 and butadiene are formed at 460°C. However, at this temperature the rate of formation of both products is constant with time over periods of many hours. If these products were formed by a reaction of butene with lattice oxygen, their rate of formation should decrease rapidly as the lattice oxygen is consumed. From the composition of the catalyst and the stoichiometry of the reaction,

$$C_4H_8 + \tfrac{1}{2}O_2 \rightarrow C_4H_6 + H_2O, \quad (1)$$

and

$$C_4H_8 + 6O_2 \rightarrow 4CO_2 + 4H_2O, \quad (2)$$

it can be calculated that at the above rate of product formation, all lattice oxygen would be depleted in 3 hrs if these products were formed by a reaction with catalyst oxygen. In one experiment over $ZnCrFeO_4$ at 460°C in the absence of oxygen using butene-2, CO_2, butadiene and butene-1 were formed at a constant rate over a 12 hr period. Activity measurements after 12 hrs showed no change in catalyst activity for oxidative dehydrogenation. Mass spectrometric analysis of the product stream over the 12-hr reaction period showed significant amounts of hydrogen formed at a constant rate. Under these conditions, the formation of butadiene, CO_2, and hydrogen can be explained by the following reactions:

$$C_4H_8 \xrightarrow{\Delta} C_4H_6 + H_2; \quad (3)$$

$$C_4H_8 \rightarrow 4'C' + 4H_2, \quad (4a)$$

and

$$4'C' + 8H_2O \rightarrow 4CO_2 + 8H_2, \quad (4b)$$

where reaction 3 is a nonoxidative catalytic dehydrogenation, and reactions 4a and 4b represent a water–gas shift in which 'C' is a carbonaceous residue, which is removed from the catalyst surface by reaction with steam. The hydrogen concentrations in the product streams are in excellent agreement with those expected from the above reac-

tions, as shown in Table 10. Therefore, in the absence of gas-phase oxygen, there is no formation of butadiene or CO_2 via bulk reduction of the zinc or magnesium–chromium ferrite catalysts.

TABLE 10
HYDROGEN CONCENTRATION IN THE PRODUCT FROM THE NONOXIDATIVE ISOMERIZATION OF BUTENE-2

Reaction time (hr)	Hydrogen concentration (mole %) calcd	Hydrogen concentration (mole %) exptl
0.5	5.03	4.96
7.0	5.43	4.96
7.5	5.49	5.19

DISCUSSION

It is generally conceded that olefin oxidative reactions over metal oxide catalysts proceed via a redox cycle, involving the reduction of at least one metal cation to a lower oxidation state by reaction with the hydrocarbon and subsequent reoxidation back to the higher oxidation state by oxygen from the gas phase. In the case of the zinc and magnesium–chromium ferrites, the redox cycle involves Fe^{+3} and Fe^{+2}, and in the absence of gas-phase oxygen the oxidative dehydrogenation of butene will not proceed once surface reduction of the catalyst has been achieved. It has been shown (*10*) that for zinc–chromium ferrite, the Fe^{+3} is not reduced beyond Fe^{+2} even under high temperature reduction in hydrogen. It was also shown that when this catalyst is reduced in butene, reduction of Fe^{+3} to Fe^{+2} occurs only to the extent that a monolayer of lattice oxygen is removed.

A reaction mechanism which is consistent with all of the experimental data obtained for the oxidative dehydrogenation of butenes over zinc–chromium ferrite would be

$$\square + C_4H_8 + Fe^{+3} + Oa^- \rightarrow (C_4H_7\text{-}Fe)^{+3} + OH^-,$$
$$(C_4H_7\text{-}Fe)^{+3} + O_L^{-2} \rightarrow C_4H_6 + Fe^{+2} + OH^-,$$
$$2OH^- \rightarrow H_2O + O_L^{-2} + \square,$$

and

$$Fe^{+2} + \tfrac{1}{2}O_2 \rightarrow Fe^{+3} + Oa^-.$$

Here $\square$ is an anion vacancy adjacent to an Fe^{+3} ion, O_a^- is an adsorbed oxygen radical ion, O_L^{-2} is a lattice oxygen, $(C_4H_7\text{-}Fe)^{+3}$ is a complex of Fe^{+3} and an allylic radical. The existence of such an allyl intermediate has been shown by Adams (*11*) and Sachtler and deBoer (*12*). The reversal of step 1 would give rise to the double-bond isomerization in the presence of gas-phase oxygen. Since in the presence of oxygen the rate of isomerization is less than the rate of dehydrogenation, then the reversal of step 1 must be slower than step 2. Either step 1 or 2 could be rate controlling.

This mechanism has four main features; (1) it does not require the reduction of an oxidation state less than Fe^{+2}; (2) in the absence of gas-phase oxygen, butadiene will be formed only until the adsorbed oxygen is consumed and there will be only a corresponding surface reduction to Fe^{+2}; (3) since either step 1 or 2 would be rate controlling, this model would predict that the formation of butadiene should be zero order in oxygen, and (4) it predicts that if reversal of step 1 is solely responsible for the double-bond isomerization, then there should be no steady-state double-bond isomerization in the absence of oxygen.

The first two points have been discussed previously and will be discussed in detail in the following paper. With respect to the third point, a complete kinetic study of the oxidative dehydrogenation of butene-2 to butadiene over $ZnCrFeO_4$ has been completed (*13*). A nonlinear regression program on a digital computer was used to fit the reaction parameters of a differential kinetic model. Numerical integration of the differential rate equation was used to fit the experimental data.

The results of this study show the rate of formation of butadiene to be zero order in both oxygen and butene over the range of conditions used for oxidative dehydrogenation. The zero-order oxygen dependence is in agreement with the proposed model. The fact that the reaction is also zero order in butene is interesting, but consistent with the model which shows a noncompetitive adsorption of butene and oxygen on two different adsorption sites.

With respect to the fourth point, it has

been shown that double-bond isomerization of butenes is faster in the absence of oxygen than when oxygen is present. It seems certain then that the isomerization in the absence of oxygen does not occur via reversal of the initial hydrogen abstraction step,

$$C_4H_8 + Fe^{+3} + O_a^- \rightleftarrows C_4H_7 - Fe^{+3} + OH^-,$$

since in the absence of oxygen neither the O_a^- nor the Fe^{+3} would be present in any significant amount in the catalyst surface. Therefore, the isomerization observed in the absence of oxygen must proceed via a route different from the elementary steps leading to dehydrogenation. The most likely mechanism for the double-bond isomerization would involve the adsorption of a butene molecule on a reduced iron (Fe^{+2}) site, followed by abstraction of a hydrogen to form an allylic radical complexed with an Fe^{+2} ion. Since this step cannot proceed to a second hydrogen abstraction, readdition of a hydrogen would result in double-bond isomerization. It is possible that isomerization occurs via this route even in the presence of oxygen, since there is a low but finite concentration of Fe^{+2} sites present during the redox cycle. In order to test this hypothesis the zinc–chromium ferrite catalyst was reduced in hydrogen under conditions at which it had been determined that most of the Fe^{+3} is reduced to Fe^{+2} (*10*).

Reactions of butene-2 were carried out over the prereduced catalyst in the absence of oxygen at 360 and 460°C under the same conditions as the experiments listed in Table 9. The results of these experiments are listed in Table 11 along with comparable data obtained on the same catalyst which was not prereduced in hydrogen. It can be seen that the extent of double-bond isomerization over the prereduced catalyst is essentially the same as the steady-state isomerization over the unreduced catalyst. It seems clear then that the isomerization, at least in the absence of oxygen, is via an interaction of butene with an Fe^{+2} site, and is in agreement with the proposed reaction model.

TABLE 11
REACTION IN THE ABSENCE OF OXYGEN OVER H_2 REDUCED $ZnCrFeO_4$

T°C	Pre-treatment	Feed	C_4H_6 (mole %)	CO_2 (mole %)	Butene-1 (mole %)
360	H_2-350°C	Butene-2	0	0	13.0
460	H_2-500°C	Butene-2	2.9	.1	25.1
460	O_2-500°C	Butene-2	3.3	.2	27.8

CONCLUSIONS

The incorporation of chromium into both the zinc and magnesium–ferrite spinel catalysts greatly increases both activity and selectivity for the oxidative dehydrogenation of butenes to butadiene. The Cr^{+3} is incorporated into octahedral sites in the spinel lattice, and inhibits the bulk reduction of the catalyst. The role of the Cr^{+3} in enhancing the catalytic activity is not completely understood at present, but it has been determined that changes in the activity are not due to the presence of a chromium-rich phase.

The formation of butadiene over these catalysts is postulated to proceed via a redox cycle involving Fe^{+3} and Fe^{+2}, with the active hydrocarbon intermediate being an allylic C_4 radical complexed with an Fe^{+3}. The active adsorbed oxygen species is postulated to be an O^- radical ion. In the absence of gas-phase oxygen, the oxidative dehydrogenation reaction ceases when the adsorbed oxygen is consumed, and there is no reaction of butene with bulk lattice oxygen to give bulk reduction of the catalyst.

ACKNOWLEDGMENTS

The authors wish to thank Mr. H. E. Lockhart and Mr. J. F. Tolley, who performed the bulk of the experiments. We are also indebted to Ameripol Incorporated, under whose sponorship a large part of this work was performed.

REFERENCES

1. KEHL, W. L., AND RENNARD, R. J., U. S. Patent 3,450,788, June 17, 1969.
2. KEHL, W. L., AND RENNARD, R. J., U. S. Patent 3,450,787, June 17, 1969.

3. WICKHAM, D. G., AND GOODENOUGH, J. B., *Phys. Rev.* **115,** 1156 (1959).
4. WALKER, L. R., WERTHEIM, G. K., AND JACCARINO, V., *Phys. Rev. Lett.* **6,** 98, (1961).
5. HANNA, S. S., HEBERLE, J., LITTLEJOHN, C., PERLOW, G. JR., PRESTON, R. S., AND VINCENT, D. H., *Phys. Rev. Lett.* **4,** 177 (1960).
6. NEEL, L., *Compt. Rend. H.* **228,** 664 (1949).
7. BEAN, C. P., AND LIVINGSTON, J. D., *J. Appl. Phys.* **30,** 1205 (1959).
8. BATIST, PH. A., KAPTEIJNS, C. A., LIPPENS, B. C., AND SCHUIT, G. C. A., *J. Catal.* **7,** 33–49 (1967).
9. WOSKOW, M. A., COLLING, P. M., KARKALITS, O. C., U. S. Patent 3,440,299, April 22, 1969.
10. MASSOTH, F. E., AND SCARPIELLO, D. A., following paper.
11. ADAMS, C. R., *Proc. Int. Cong. Cata. 3rd, A. 1964* **1,** 240 (1965).
12. SACHTLER, W. H. M., AND DEBOER, N. H., *Proc. Int. Congr. Catal., 3rd, A. 1964* **1,** 252 (1965).
13. STERRETT, J. S., unpublished manuscript.